1-1-2014

Graphene cryogel papers with enhanced mechanical strength for high performance lithium battery anodes

Kewei Shu
University of Wollongong, ks323@uowmail.edu.au

Caiyun Wang
University of Wollongong, caiyun@uow.edu.au

Meng Wang
University of Wollongong, mw088@uowmail.edu.au

Chen Zhao
University of Wollongong, cz995@uowmail.edu.au

Gordon G. Wallace
University of Wollongong, gwallace@uow.edu.au

Graphene cryogel papers with enhanced mechanical strength for high performance lithium battery anodes

Abstract

A porous graphene paper was prepared by pressing a graphene cryogel, followed by thermal reduction at 220 °C. The cryogel was formed by freeze-drying a solution containing chemically reduced graphene and graphene oxide (CRG/GO). The formed graphene cryogel papers deliver a much higher discharge capacity and rate capability than that from conventional graphene papers fabricated by filtration. These new structures have a discharge capacity higher than 400 mA h g−1 at a current density of 2000 mA g−1 in sharp contrast to 229 mA h g−1 at 50 mA g−1 obtained from conventional graphene papers. These greatly improved electrochemical properties may be attributed to the porous structure and the concomitant high surface area. The mechanical properties may be tuned with the CRG/GO ratio. At a CRG/GO mass ratio of 2:1 the graphene paper has a Young's modulus nearly 9 times greater than an equivalent paper made from pure GO.

Keywords

anodes, performance, graphene, cryogel, battery, papers, lithium, enhanced, mechanical, strength, high

Disciplines

Medicine and Health Sciences | Social and Behavioral Sciences

Publication Details

Shu, K., Wang, C., Wang, M., Zhao, C. & Wallace, G. G. (2014). Graphene cryogel papers with enhanced mechanical strength for high performance lithium battery anodes. Journal of Materials Chemistry A, 2 (5), 1325-1331.

Graphene Cryogel Paper with Enhanced Mechanical Strength for High Performance Lithium Battery Anode

Kewei Shu, Caiyun Wang*, Meng Wang, Chen Zhao, Gordon Wallace*

A porous graphene paper was prepared by pressing a graphene cryogel, followed by thermal reduction at 220°C. The cryogel was formed by freeze-drying a solution containing chemically reduced graphene and graphene oxide (CRG/GO). The formed graphene cryogel papers deliver a much higher discharge capacity and rate capability than that from conventional graphene papers fabricated by filtration. These new structures have a discharge capacity higher than 400 mAh g^{-1} at a current density of 2000 mA g^{-1} in sharp contrast to the 229 mAh g^{-1} at 50 mA g^{-1} obtained from conventional graphene papers. These greatly improved electrochemical properties may be attributed to the porous structure and the concomitant high surface area. The mechanical properties may be tuned with the CRG/GO ratio. At a CRG/GO mass ratio of 2:1 the graphene paper has a Young's modulus nearly 9 times greater than an equivalent paper made from pure GO.

1. Introduction

Nowadays, increasing interests is being aroused in portable electronic devices including roll-up display, implantable and wearable medical devices.[1-3] As the indispensable components, flexible energy conversion and storage units with high energy and power density are required.[4, 5] The electrodes used in such energy system should possess the superior electrochemical properties along with the mechanical flexibility. Free-standing paper-like materials are the promising electrodes of interest, which normally include carbon-based and electrically conducting polymers (ECPs) based material.[5, 6] They are flexible and mechanically strong, which can be easily moulded and shaped into the desired structures. Also they can be used directly without the use of low capacity conducting additives and insulating binder, thus leading to high energy and power density.

Free-standing carbon nanotube (CNT) buckypaper can be easily fabricated by filtration method from its dispersion. It demonstrates promising electrochemical properties as either a battery or supercapacitor electrode due to its porous structure formed with the entangled nanotubes facilitating the efficient ion transport.[7-10] In addition, ECPs[11] and metal oxides[12, 13] are introduced to form CNT composite papers to further improve its charge capacity. The flexible ECPs or ECPs composite paper electrode has also been extensively studied for flexible energy storage application.[14, 15]

Compared with CNTs and ECPs, graphene possesses the advantages of high specific surface area and excellent electronic transport properties. It has been extensively investigated as battery or supercapacitor materials offering excellent electrochemical properties – high energy and power densities.[16-19] The flexible graphene or graphene oxide (GO) paper can also be easily fabricated by flow-directed graphene nanosheets assembly,[20, 21] and superior electrochemical properties are expected as that from the graphene powder.[16-19, 22] However, its performance was far from satisfactory. It delivered a very low reversible discharge capacity of 84 mAh g^{-1} at a current density of 50 mA g^{-1}, and the reversible capacity increased to 301 mAh g^{-1} after removing some oxygen-contained functional group in our previous report.[23] It can be explained that the aggregation or restacking of the graphene nanosheets due to the strong π-π stacking and van der Waals forces, which limits the available surface area and retards its electrochemical properties.

To obtain a porous/uncompact graphene paper with high charge capacity, several strategies such as leavening, template-directed assembly and cavitation-chemical oxidation are applied.[24-26] The "wet" graphene paper with solvents as the spacer preventing the graphene nanosheets restacking[27] delivered a specific capacitance of 156.5 F g^{-1} at an ultrafast charge-discharge rate of 1080 A g^{-1}. Graphene paper with open pores can also be formed with the cavity due to gas release during the chemical reduction of GO paper. Such paper delivered a greatly improved

specific capacitance of 110 F g^{-1} at 0.5 A g^{-1} in comparison with that of 17 F g^{-1} for highly packed graphene paper.[24] By using polymer microspheres as the template, a macroporous graphene paper with controlled pore size was fabricated by flow-directed self-assembly method. The macroporous graphene paper exhibits an electrochemical capacitance of 49.2 F g^{-1} at 3.0 A g^{-1}.[26]

More recently, a folded structure graphene paper was made from a freeze-dried GO cryogel and the subsequent thermal reduction. It presented significantly improved performances in lithium batteries compared to the graphene paper by filtration method, which can maintain reversible capacity of 568 mAh g^{-1} at 100 mA g^{-1} after 100 cycles.[28] However, this paper was brittle and fragile due to its loose-packed layered structure. The thermal reduction of such GO cryogel paper further deteriorates its mechanical properties.

In this work, we introduce chemically reduced graphene (CRG) into the GO dispersion as the precursor solution for making the graphene cryogel. CRG possesses much less functional groups than GO. The introduction of CRG can decrease the entrapped water content associated to H bond in the formed graphene cryogel, which are expected to result in cryogel with better mechanical properties. The rationale is that the mechanical properties of graphene paper were essentially controlled by H-bond networks which strength can be enhanced with decreased water content within the interlayer cavities.[29] Our results clearly demonstrate that the mechanical properties of the graphene paper are remarkably enhanced with the increasing ratio of CRG. In addition, those CRG/GO hybrid papers all display excellent performance as anode in lithium ion battery, especially at high current densities.

2. Experimental

2.1 Material synthesis

Graphite oxide was synthesized from natural graphite flakes by the modified Hummels method.[30, 31] Exfoliation of graphite oxide to graphene oxide (GO) was achieved by ultrasonication of the dispersion using a Brandson Digital Sonifier (S450D, 30% amplitude, 2s on, 1s off) for 30 min. Chemically reduced graphene (CRG) aqueous solution was prepared by reduction of GO solution using hydrazine in presence of ammonium solution,[32] and it is described briefly as follows. 168 μL of ammonium solution (28 wt%) and 216 μL of hydrazine solution (35% in water) were added into 40 mL 1.5 mg mL^{-1} GO dispersion while stirring. The resultant mixture was then stirred at 95°C for 1h to complete the reduction. The as-prepared CRG solution was diluted to give a 1 mg mL^{-1} and 0.4 mg mL^{-1} solution. The CRG/GO precursor hybrid solution was obtained by directly stir-mixing the GO and CRG solution. The CRG/GO mass ratio used in this work is 1:5, 1:2 and 2:1. The resultant hybrid solution was transferred into a 50 ml beaker and subjected to a freezing-dry process to form a cryogel, which included an 8 h frozen at -30°C and a 36 h freeze-drying. The hybrid (CRG/GO) papers were obtained by pressing the cryogels at 20 MPa, and named as GO-CRG-0.5, GO-CRG-2 and GO-CRG-5 according to the mass ratio of GO to CRG. The graphene (rGO) papers were obtained using the thermal reduction of the GO or hybrid papers at 220°C in air for 2h. Correspondingly, they are named as rGO-CRG-0.5, rGO-CRG-2 and rGO-CRG-5, respectively. A pure rGO paper was also prepared using the same method for comparison. In addition, graphene paper was also prepared by filtration of 60mL 0.4 mg mL^{-1} CRG solution.

2.2 Material characterization

Conductivity measurements were carried out on a JandelRM3 Conductivity Meter using a four-point probe method. The morphology was investigated using a field-emission scanning electron microscope (FESEM, JEOL JSM7500FA). XRD measurements were performed on an Australia GBC Scientific X-ray diffract meter (Cu K_α radiation, λ=1.5418 A˚) with a scan rate of 2° min^{-1}. Raman spectra were obtained using a confocal Raman spectrometer (Jobin Yvon HR800, Horiba) utilizing 632.8 nm diode lasers. The thermal properties were characterized by TGA (Q500, TA instruments), and the measurements were tested under nitrogen with a ramp rate of 5°C min^{-1}. Uniaxial in-plane tensile tests were studied using a Shimadzu EZ mechanical tester. The samples with a dimension of approximately 3×15 mm^2 were used for mechanical testing at a cross head speed of 1mm min^{-1}.

2.3 Electrochemical properties

The graphene papers were assembled into LR 2032 type coin cells coupled with lithium metal anode for electrochemical properties testing. The electrolyte used was 1M $LiPF_6$ in 1:1 (v/v) ethylene carbonate/dimethyl carbonate. Galvanostatic charge/discharge tests were performed using a LAND CT2001A battery test system (Wuhan Jinnuo Electronics Co. Ltd. China) over a potential range of 0.005–3.0 V (vs. Li/Li^+). Cyclic voltammetry of the cells was tested using a Solartron SI 1287 and scanned between 0.0 to 3.0 V (vs. Li/Li^+) at a rate of 0.1 mV s^{-1}. Electrochemical impedance spectroscopy (EIS) measurements were performed using a Gamry EIS 3000 system, and the frequency range spanned from 100 kHz to 0.01 Hz with amplitude of 10 mV at open circuit potential.

3. Results and discussion

The as-prepared cryogel shows an interconnected three-dimensional porous network (Fig. 1a) with the pore wall composed of graphene sheets. The pore is formed due to the sublimation of ice crystal during the freeze drying process, and its size is in the range of tens of micrometers

to submillimeters. The graphene cryogel paper can be easily obtained by pressing the cryogel at 20 MPa, and followed by thermal annealing at 220°C for 2h in air. The thickness of all the graphene papers is around 20 μm with a conductivity of approximately 2-5 S cm^{-1}. For all the cryogel papers have the similar structure (i.e. similar surface morphology and cross-sectional view), only that of the rGO-CRG-0.5 cryogel paper is presented here. Figure 1c shows the surface morphology of the graphene paper. Different from the smooth surface of that graphene paper fabricated by flow-directed filtration (Figure 1e), our graphene paper exhibits a rough surface containing graphene folds with random size (Figure 1c). A loosely-packed layered structure can be observed through the cross-sectional view of our graphene paper (Figure 1d), in comparison with the compacted graphene layers structures for graphene paper formed by filtration (Figure 1f).

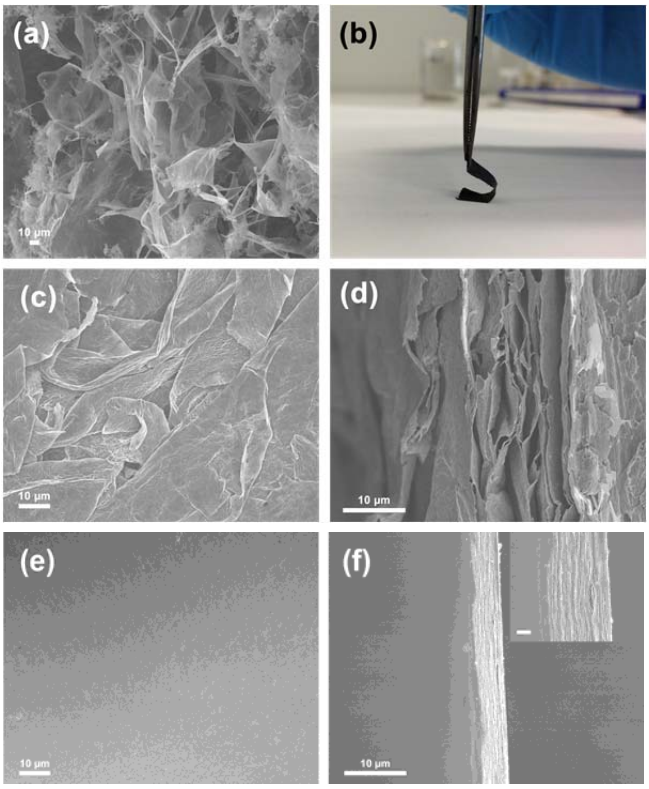

Figure 1 (a) FESEM image of rGO-CRG-0.5 cryogel; (b) Photograph of rGO-CRG-0.5 paper demonstrating its flexibility. FESEM images of the surface morphology and cross section of rGO-CRG-0.5 paper (c, d) and CRG paper by filtration (e, f). (Inset, cross-sectional view of f at higher magnification. Scale bar: 1 μm.)

X-ray diffraction (XRD) patterns of the hybrid paper and GO paper before and after reduction are shown in Figure 2A. GO paper displayed a strong and sharp peak at 9.8° (2θ), as reported for GO solids and GO paper.[33, 34] This strong diffraction derives from the interspacing between the stacking layers of GO sheets, which corresponds to a d-spacing of ~ 0.91 nm. After thermal reduction, a broad peak at 24° (2θ) is presented for rGO paper, which corresponding to an average interlayer spacing of 0.37 nm. Compared to GO paper, the hybrid papers displayed two peaks, close to 10° and 24°. The former belongs to (0 0 2) diffraction of GO and the latter can be ascribed to (0 0 2) diffraction of rGO. The (002) peak intensity decreased correspondingly with the decreased GO content in this hybrid. For GO-CRG-5 paper, there is no pronounced rGO peak due to its low content. The Raman spectra of CRG, GO-CRG-0.5, GO-CRG-2, GO-CRG-5 and GO paper with normalized intensity is shown in Figure 2B. They all display a typical G band (1588 cm^{-1}) and D band (1334 cm^{-1}), corresponding to the first order scattering of the E_{2g} mode (G band) and disordered structures (D band), respectively.[35] The D/G intensity ratio is 1.22 for GO, and then increases to 1.59 after chemically reduction (CRG). The change of D/G ratio can be attributed to the decrease in the average size of the sp^2 domains upon reduction process.[36] The new graphitic domains in CRG are increased in number but smaller in size. The D/G ratio for GO-CRG-5, GO-CRG-2, GO-CRG-0.5 is 1.29, 1.35 and 1.45 respectively, which agrees well with the CRC ratio increase.

The TGA curves of the graphene paper with different CRG/GO ratio are shown in Figure 2C. The weight loss below 100 °C can be attributed to the evaporation of absorbed water. The hydrophilic GO paper demonstrated a substantial loss of approximately 10% in this temperature range. The major weight loss of the GO paper occurs near 150°C, which may be caused by pyrolysis of oxygen-containing groups from the GO surface.[34] In the temperature range between 100-200°C, which is mainly the decomposition of oxygen-containing groups on GO in those hybrid papers, the weight loss are 25%, 17%, 13% and 7% for GO, GO-CRG-5, GO-CRG-2, GO-CRG-0.5. Such decreased weight loss in this temperature range agrees with the decreased content of GO in the hybrid papers. For all of the papers, the weight loss in the temperature range between 200 °C and 500 °C is about 10%, which probably due to the decomposition of some residual oxygen-containing groups.[21] The total weight loss between 100°C to 600°C for rGO, GO-CRG-0.5, GO-CRG-2, GO-CRG-5 and rGO are 9%, 14%, 30%, 35% and 53%.

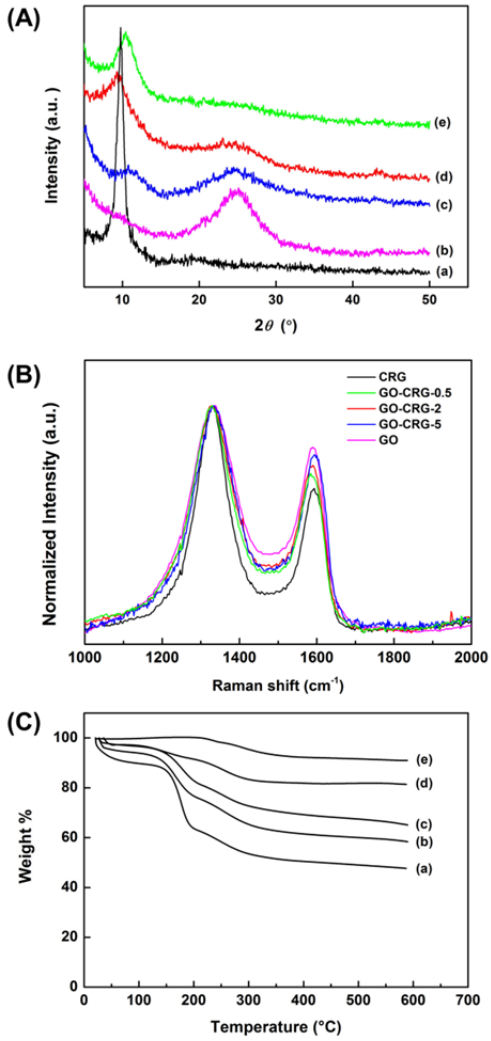

Figure 2 (A) XRD patterns of GO paper (a), rGO paper (b), hybrid papers of GO-CRG-0.5 (c), GO-CRG-2 (d) and GO-CRG-5 (e). (B) Raman spectra of all graphene papers with normalized intensity. (C) TGA curves of graphene papers with different CRG/GO ratio: (a), pure GO; (b), GO-CRG-5; (c), GO-CRG-2; (d), GO-CRG-0.5; and (e) rGO.

The mechanical properties were tested in uniaxial tension of our graphene papers strips. The stress-strain response of graphene papers with different CRG/GO ratio is shown in Figure 3. These curves show straightening behavior at the beginning followed by roughly linear behavior and then plastic deformation behavior, similar to graphene paper fabricated by filtration method.[20] The ultimate tensile strain for the hybrid graphene papers is 1.5 %, twice as much as the value of rGO paper (0.75 %). The Young's modulus can be calculated from the initial slope of the stress strain curve, and it was 58, 92, 179 and 510 MPa for rGO, rGO-CRG-5, rGO-CRG-2 and rGO-CRG-0.5, respectively. It can be clearly seen that the mechanical properties of our graphene papers are improved with the increasing aspect ratio of CRG. The increase of mechanical strength is resulted from to lower water content integrated with the hydrophobic CRG sheets compared with hydrophilic GO sheets. It is believed that lower water content in graphene papers leads to better H-bond networks making the graphene paper stiffer.[29] In addition, the hybrid paper with higher GO content may also suffer from the structural destruction caused by pyrolysis of oxygen-containing groups from the GO during thermal reduction, resulting in poorer mechanical properties. We should also point out that our graphene paper presents much lower modulus compared to flow-directed assembled graphene paper,[20] which can be ascribed to their loosely packed structure.

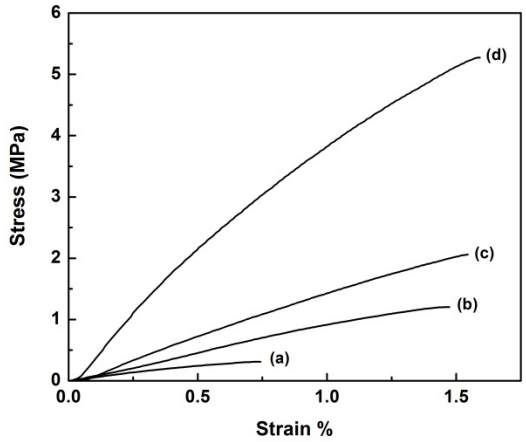

Figure 3 Stress-strain curves of graphene papers with different CRG/GO ratio: (a) rGO; (b) rGO-CRG-5; (c) rGO-CRG-2; and (d) rGO-CRG-0.5.

The electrochemical properties of our graphene papers as binder-free electrode for lithium batteries are evaluated by galvanostatic charge/discharge in the potential range from 0.005 to 3.0 V. All of the graphene cryogel papers exhibit much similar performance, so here we only present rGO, rGO-CRG-0.5 cryogel paper and filtrated CRG paper for easy comparison. They all presented an irreversible capacity between the first and second discharge cycle. The irreversible capacity near 0.5V is attributed to the formation of a solid electrolyte interface (SEI) layer in the first cycle. The reversible capacity below 0.5 V should be due to the lithium binding on the basal plane of the graphene sheets. While the capacity between 0.5-1.5 V may be ascribed to the faradic capacitance on the surface or on the edge sites of graphene sheets.[19] The first and second cycle charge/discharge profiles of hybrid paper electrode rGO-CRG-0.5 at current density of 50 mA g^{-1} are shown in Figure 4a. It delivers a first discharge capacity of 903 mAh g^{-1}, then the discharge capacity drops to 642 mAh g^{-1} on the second cycle. The Coulombic efficiency of our graphene papers is about 60-70% during the initial charge/discharge cycle similar to the performance of graphene powder.[23, 33, 37] This hybrid graphene cryogel paper exhibits a much higher reversible capacity compared to other paper based carbon materials. The reversible capacity of our graphene cryogel paper is at least 10 times

higher than that of flexible graphite foil, only 50 mAh g^{-1} obtained at C/20 rate (18.6 mA g^{-1}).[38] Also it is even higher than that of 6-15 layered graphene nanosheets, which shows a 540 mAh g^{-1} at the same current density.[19] The graphene paper obtained by filtration shows second discharge capacity of 229 mAh g^{-1} at the same current density (Figure 4b), only half the value compared to our cryogel paper. The porous and loose-packed structure in our graphene paper may prevent the restacking of the graphene nanosheet, also provides more lithium insertion active sites thus leads to a higher reversible capacity. The rGO-CRG-0.5 paper shows equivalent performance to that of rGO cryogel paper (Figure 4c), which has a second discharge capacity of 600 mAh g^{-1}, indicates the electrochemical performance of the cryogel paper is not affected by introduction of CRG.

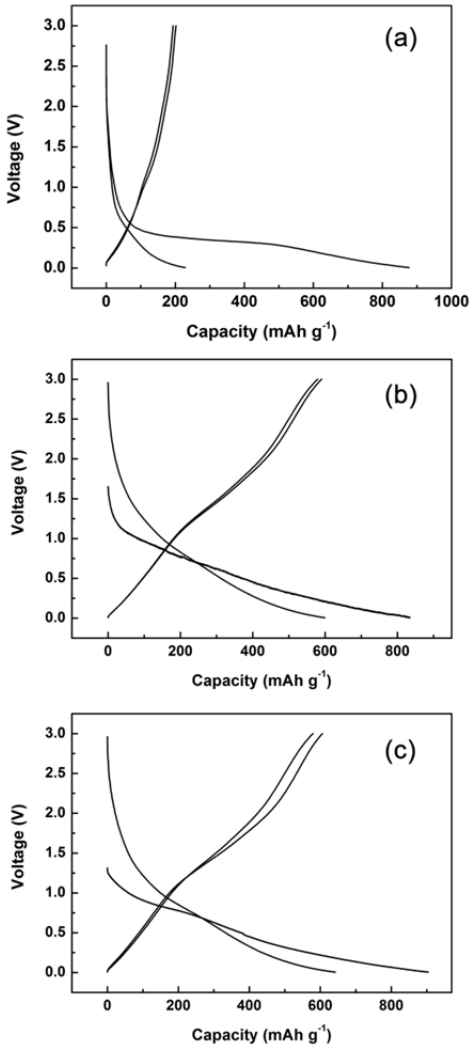

Figure 4 First and second charge discharge curves of graphene papers: (a) rGO-CRG-0.5 (b) CRG by filtration (c) rGO.

Figure 5a, 5b presents the charge/discharge profiles of graphene cryogel papers at higher current densities. The performance of graphene paper (filtration) electrode at higher current densities is not shown here due to it very low discharge capacity even at a low discharge current density of 50 mA g^{-1}. As can be clearly seen from the figure, such graphene papers possess high rate discharge/charge capability. For rGO-CRG-0.5 paper (Figure 5b), at the current densities of 200, 500, 1000, 2000 and 3000 mA g^{-1}, the corresponding reversible capacity can reach 622, 557, 485, 405 and 355mAh g^{-1} respectively. The performance of rGO-CRG-0.5 is very close to that of rGO paper, which shows reversible capacity of 596, 537, 471, 403 and 357mAh g^{-1}, respectively (Figure 5a). The high rate discharge/charge properties are likely to originate in the easy accessibility and transportation of electrolyte into the host position of the graphene sheets due to the folded and porous structure of our graphene paper. They also displayed a good cyclic performance and reversibility (Figure 5c, 5d). After 100 cycles at a current density of 2000 mA g^{-1}, the rGO-CRG-0.5 paper and rGO paper still maintains a specific capacity of 395 mAh g^{-1} and 394 mAh g^{-1}, 98.7% and 98.9% of the initial capacity.

The cyclic voltammograms (CV) of the rGO-CRG-0.5 cryogel paper, rGO cryogel paper and graphene paper are shown in Figure 6a, b and c. They all exhibit much similar current responses in electrochemical window of 0.0 V to 3.0 V versus Li/Li^+. The cathodic peak around 0.5V indicates the formation of SEI. A large irreversible cathodic peak corresponds to lithium intercalation appeared around 0.0 V, which became weaker after the first cycle due to the lithium intercalation reaction being partially reversible. The cathodic peak at about 1.5 V is attributed to lithium interactions with the residual functional groups on the surface or on the edge sites of graphene sheets. The shape of the CV curves matches well with the discharge/charge profiles.

Electrochemical impedance spectroscopy was used to evaluate the filtrated graphene paper and the graphene cryogel paper electrodes after several cycles (Figure 6d) in the Nyquist plot. The semicircle in the medium frequency region is related to the charge-transfer reaction of lithium intercalation into graphene sheets, and the inclined line at an approximate 45° angle to the real axis corresponds to the lithium-diffusion process within carbon electrodes.[39] It can be clearly seen from the EIS curves, the diameter of the semicircle at the medium frequency region of the graphene cryogel papers is significantly reduced compared to the graphene paper obtained by filtration, indicative of a lower charge-transfer resistance in the graphene cryogel papers. The reduced charge transfer resistance might be induced by the easy accessibility and transportation of electrolyte in the loose packed structure.

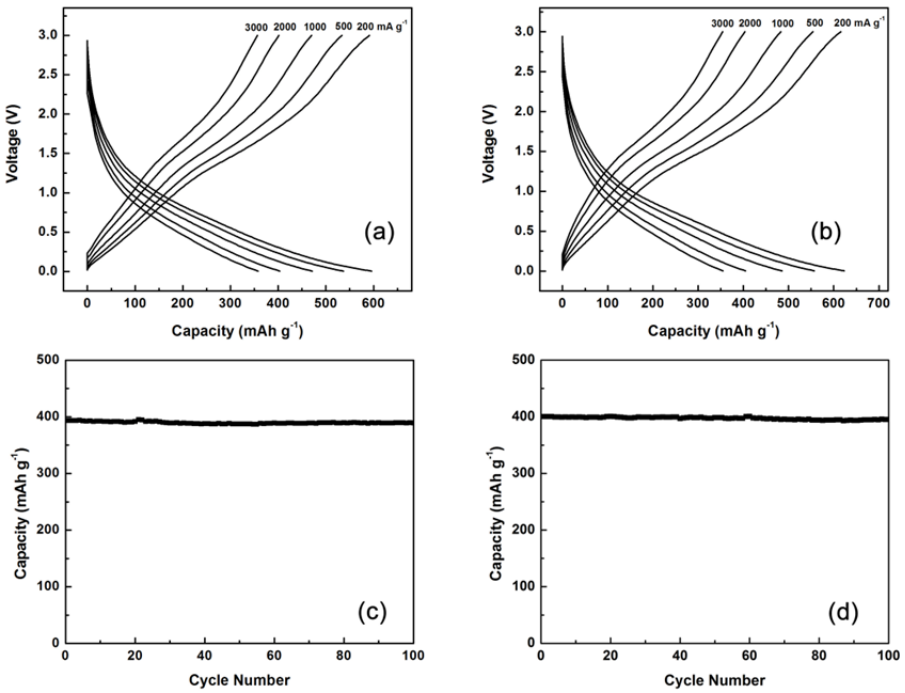

Figure 5 Charge discharge curves of graphene papers at different current densities: (a) rGO (b) GO-CRG-0.5. Capacity versus cycle number at 2000 mA g^{-1}: (c) rGO (d) rGO-CRG-0.5.

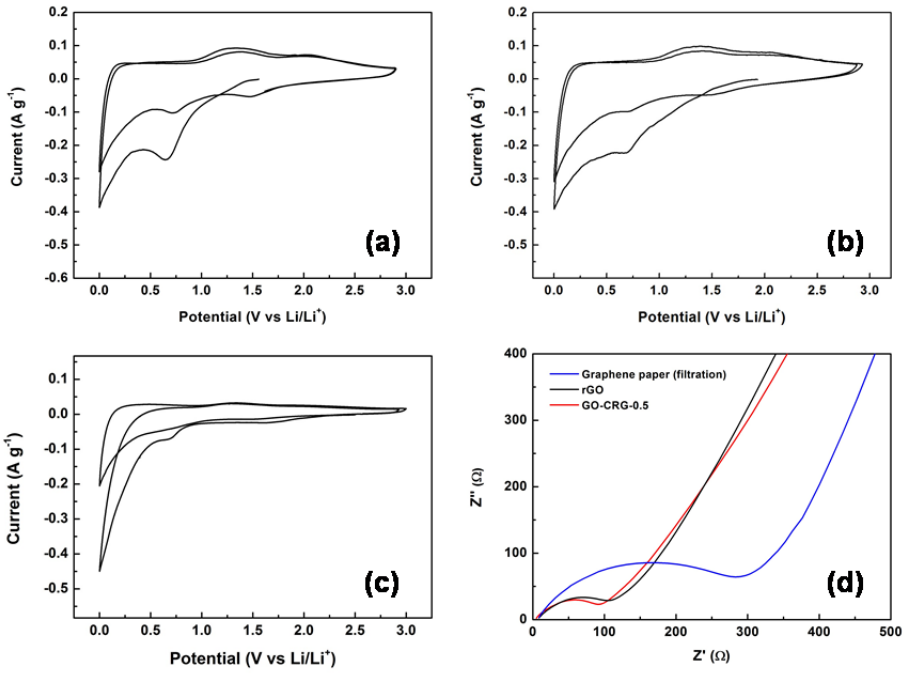

Figure 6 Cyclic voltammograms obtained for graphene papers using a scan rate of 0.1 mV s^{-1}: (a) rGO-CRG-0.5 (b) rGO (c) graphene paper. (d) Nyquist plots of graphene cryogel papers and the graphene papers (filtration).

Conclusions

In summary, flexible graphene paper with a porous structure has been fabricated by mechanically pressing a graphene cryogel, prepared from a precursor solution containing different CRG/GO ratios. The mechanical property of such graphene papers was significantly enhanced with the increase of the CRG/GO ratio in the precursor solution. The introduction of CRG in the precursor solution resulted in a strong graphene paper

without sacrificing electrochemical performance. All electrodes prepared exhibited enhanced electrochemical properties (high discharge capacity, good rate capability and cycling stability) compared to that graphene paper fabricated by filtration. The improved performance is attributed to the easy accessibility and transportation of electrolyte in the loose packed structures. This novel flexible/bendable graphene electrode should find use in flexible energy storage devices.

Acknowledgements

The authors thank the Australian Research Council (ARC) for financial support under the ARC Centre of Excellence for Electromaterials Science, and the ANFF Materials Node for their provision of research facilities. Kewei Shu and Chen Zhao acknowledge the support of the CSC scholarship from the Ministry of Education of P. R. China. The authors also acknowledge the use of facilities within UOW Electron Microscopy Centre.

Notes and references

Intelligent Polymer Research Institute, ARC Centre of Excellence for Electromaterials Science, AIIM Facility, Innovation Campus, University of Wollongong, Wollongong, NSW 2522 Australia.
*Tel: +61 2 42981426. Fax: +61 2 4221 3124. E-mail: caiyun@uow.edu.au (C.W.).
Tel: +61 2 42213127. Fax: +61 2 42213124. E-mail: gwallace@uow.edu.au (G.G.W.).

1. J. A. Rogers, Z. Bao, K. Baldwin, A. Dodabalapur, B. Crone, V. R. Raju, V. Kuck, H. Katz, K. Amundson, J. Ewing and P. Drzaic, *Proc. Natl. Acad. Sci. U. S. A.*, 2001, **98**, 4835-4840.
2. S. R. Forrest, *Nature*, 2004, **428**, 911-918.
3. T. Someya, T. Sekitani, S. Iba, Y. Kato, H. Kawaguchi and T. Sakurai, *Proc. Natl. Acad. Sci. U. S. A.*, 2004, **101**, 9966-9970.
4. H. Nishide and K. Oyaizu, *Science*, 2008, **319**, 737-738.
5. V. L. Pushparaj, M. M. Shaijumon, A. Kumar, S. Murugesan, L. Ci, R. Vajtai, R. J. Linhardt, O. Nalamasu and P. M. Ajayan, *Proc. Natl. Acad. Sci. U. S. A.*, 2007, **104**, 13574-13577.
6. L. Nyholm, G. Nystrom, A. Mihranyan and M. Stromme, *Advanced Materials*, 2011, **23**, 3751-3769.
7. S. H. Ng, J. Wang, Z. P. Guo, G. X. Wang and H. K. Liu, *Electrochim. Acta*, 2005, **51**, 23-28.
8. B. J. Landi, M. J. Ganter, C. M. Schauerman, C. D. Cress and R. P. Raffaelle, *The Journal of Physical Chemistry C*, 2008, **112**, 7509-7515.
9. M. Kaempgen, J. Ma, G. Gruner, G. Wee and S. G. Mhaisalkar, *Appl. Phys. Lett.*, 2007, **90**.
10. C. M. Niu, E. K. Sichel, R. Hoch, D. Moy and H. Tennent, *Appl. Phys. Lett.*, 1997, **70**, 1480-1482.
11. J. Chen, Y. Liu, A. I. Minett, C. Lynam, J. Z. Wang and G. G. Wallace, *Chemistry of Materials*, 2007, **19**, 3595-3597.
12. L. Noerochim, J.-Z. Wang, S.-L. Chou, D. Wexler and H.-K. Liu, *Carbon*, 2012, **50**, 1289-1297.
13. L.-F. Cui, L. Hu, J. W. Choi and Y. Cui, *Acs Nano*, 2010, **4**, 3671-3678.
14. A. Mihranyan, L. Nyholm, A. E. G. Bennett and M. Stromme, *Journal of Physical Chemistry B*, 2008, **112**, 12249-12255.
15. G. Nystrom, A. Razaq, M. Stromme, L. Nyholm and A. Mihranyan, *Nano Letters*, 2009, **9**, 3635-3639.
16. A. Peigney, C. Laurent, E. Flahaut, R. R. Bacsa and A. Rousset, *Carbon*, 2001, **39**, 507-514.
17. S. V. Morozov, K. S. Novoselov, M. I. Katsnelson, F. Schedin, D. C. Elias, J. A. Jaszczak and A. K. Geim, *Physical Review Letters*, 2008, **100**.
18. M. D. Stoller, S. J. Park, Y. W. Zhu, J. H. An and R. S. Ruoff, *Nano Letters*, 2008, **8**, 3498-3502.
19. E. Yoo, J. Kim, E. Hosono, H. Zhou, T. Kudo and I. Honma, *Nano Letters*, 2008, **8**, 2277-2282.
20. D. A. Dikin, S. Stankovich, E. J. Zimney, R. D. Piner, G. H. B. Dommett, G. Evmenenko, S. T. Nguyen and R. S. Ruoff, *Nature*, 2007, **448**, 457-460.
21. H. Chen, M. B. Mueller, K. J. Gilmore, G. G. Wallace and D. Li, *Advanced Materials*, 2008, **20**, 3557-3561.
22. S. Park, K.-S. Lee, G. Bozoklu, W. Cai, S. T. Nguyen and R. S. Ruoff, *Acs Nano*, 2008, **2**, 572-578.
23. C. Wang, D. Li, C. O. Too and G. G. Wallace, *Chemistry of Materials*, 2009, **21**, 2604-2606.
24. Z. Niu, J. Chen, H. H. Hng, J. Ma and X. Chen, *Advanced Materials*, 2012, **24**, 4144-4150.
25. X. Zhao, C. M. Hayner, M. C. Kung and H. H. Kung, *Acs Nano*, 2011, **5**, 8739-8749.
26. C.-M. Chen, Q. Zhang, C.-H. Huang, X.-C. Zhao, B.-S. Zhang, Q.-Q. Kong, M.-Z. Wang, Y.-G. Yang, R. Cai and D. Sheng Su, *Chemical Communications*, 2012, **48**, 7149-7151.
27. X. Yang, J. Zhu, L. Qiu and D. Li, *Adv. Mater.*, 2011, **23**, 2833-2838.
28. F. Liu, S. Song, D. Xue and H. Zhang, *Advanced Materials*, 2012, **24**, 1089-1094.
29. N. V. Medhekar, A. Ramasubramaniam, R. S. Ruoff and V. B. Shenoy, *Acs Nano*, 2010, **4**, 2300-2306.
30. W. S. Hummers and R. E. Offeman, *Journal of the American Chemical Society*, 1958, **80**, 1339-1339.
31. S. Park, J. H. An, R. D. Piner, I. Jung, D. X. Yang, A. Velamakanni, S. T. Nguyen and R. S. Ruoff, *Chemistry of Materials*, 2008, **20**, 6592-6594.
32. D. Li, M. B. Muller, S. Gilje, R. B. Kaner and G. G. Wallace, *Nat Nano*, 2008, **3**, 101-105.
33. A. Abouimrane, O. C. Compton, K. Amine and S. T. Nguyen, *J. Phys. Chem. C*, 2010, **114**, 12800-12804.
34. O. C. Compton, D. A. Dikin, K. W. Putz, L. C. Brinson and S. T. Nguyen, *Advanced Materials*, 2010, **22**, 892-896.
35. F. Tuinstra and J. L. Koenig, *The Journal of Chemical Physics*, 1970, **53**, 1126-1130.
36. S. Stankovich, D. A. Dikin, R. D. Piner, K. A. Kohlhaas, A. Kleinhammes, Y. Jia, Y. Wu, S. T. Nguyen and R. S. Ruoff, *Carbon*, 2007, **45**, 1558-1565.
37. G. X. Wang, X. P. Shen, J. Yao and J. Park, *Carbon*, 2009, **47**, 2049-2053.
38. M. S. Yazici, D. Krassowski and J. Prakash, *Journal of Power Sources*, 2005, **141**, 171-176.
39. T. Piao, S. M. Park, C. H. Doh and S. I. Moon, *Journal of The Electrochemical Society*, 1999, **146**, 2794-2798.

Graphitic Abstract

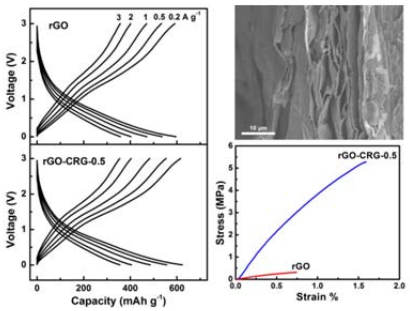

The mechanical properties of graphene paper can be tuned with CRG/GO ratio, demonstrating high performance in lithium batteries.